

Supporting information

Materials and instrumentation

All reagents were purchased from Sigma-Aldrich and Merck chemical companies and used without further purification. FT-IR spectra were recorded on a Bruker Tensor 27 FT-IR spectrophotometer using KBr pellets over the range of 4000–400 cm⁻¹. The X-ray powder diffraction (XRD) data were recorded on a Siefert XRD 3003 PTS diffractometer, using Cu K_{α1} radiation ($\lambda = 1.5406 \text{ \AA}$). UV-Vis spectra were obtained with a shimadzu UV-260 spectrophotometer. Scanning electron microscopy (SEM) images were obtained on a Philips XL-30ESEM equipped with an X-ray energy dispersive detector. Thermogravimetric analysis (TGA) was performed using a Mettler Toledo TGA/DSC instrument with heating rate of 10 °C/min in an air atmosphere. Nitrogen sorption isotherms were recorded on a Belsorp Mini-II instrument at 77K. The amount of sulfur was determined using an ELTRA carbon-sulfur analyzer.

Adsorption kinetics

The pseudo-first-order is based on the following equation:

$$\log(q_e - q_t) = \log q_e - \frac{k_1}{2.303}t \quad (1)$$

Where q_e and q_t (mg/g) are the amounts of dye adsorbed at equilibrium and contact time (t), respectively and K_1 (min⁻¹) represents the rate constant of pseudo-first-order kinetics.

The pseudo-second-order model is generally represented as follows:

$$\frac{t}{q_t} = \frac{1}{k_2 q_e^2} + \frac{1}{q_e} t \quad (2)$$

Where K_2 (g.mg⁻¹ min⁻¹) denotes the adsorption constant of pseudo-second-order kinetics.

Adsorption isotherms

The Langmuir isotherm is expressed by the following equation:

$$\frac{c_e}{Q_e} = \frac{1}{Q_{max}} + \frac{1}{k_L Q_{max}} \quad (3)$$

Where C_e is the equilibrium concentration of the dye in the solution (mg.g^{-1}), Q_e represents the amount of the adsorbed dye at equilibrium (mg/g), Q_{max} denotes the maximum adsorption capacity (mg/g), and K_L is the Langmuir constant (L/g) which is related to the adsorption binding energy. The Freundlich model is represented as:

$$\ln Q_e - \ln k_F = \frac{1}{n} \ln C_e \quad (4)$$

Where K_F and n are Freundlich adsorption constants which are attributed to the heterogeneous surface of the adsorbent and the desirability of the adsorption, respectively. If n is greater than 1, the adsorption is favorable and in the case of $n < 1$, the adsorption is unfavorable.

Adsorption thermodynamics

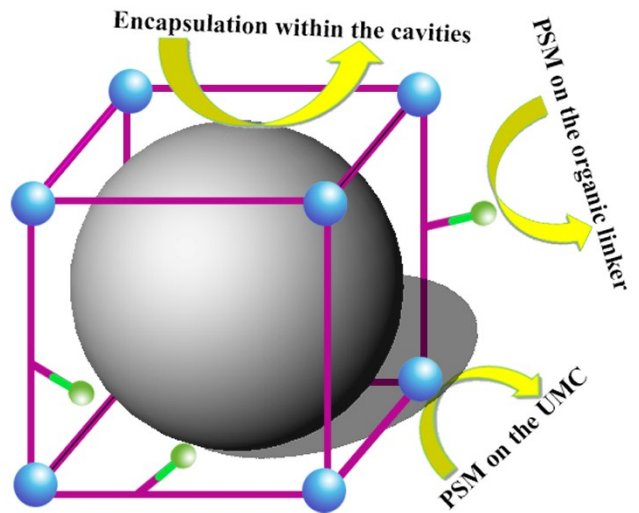
The values of thermodynamic parameters including the changes in enthalpy (ΔH° ; kJ/mol), entropy (ΔS° ; kJ/mol), and Gibbs free energy (ΔG° ; kJ/mol) were computed by the following equations:

$$\ln K_0 = \frac{\Delta S^\circ}{R} - \frac{\Delta H^\circ}{RT} \quad (5)$$

$$-RT \ln K_0 = \Delta H^\circ - T \Delta S^\circ \quad (6)$$

$$\Delta G^\circ = \Delta H^\circ - T \Delta S^\circ \quad (7)$$

Where K_0 is the thermodynamic equilibrium constant, T is the solution temperature (K), and R is the universal gas constant (8.314 J/mol.K) and the plots of $\ln K_0$ vs. $1/T$ are shown in Fig. S14.



Scheme S1. Various situation for post synthetic modification of MOFs.

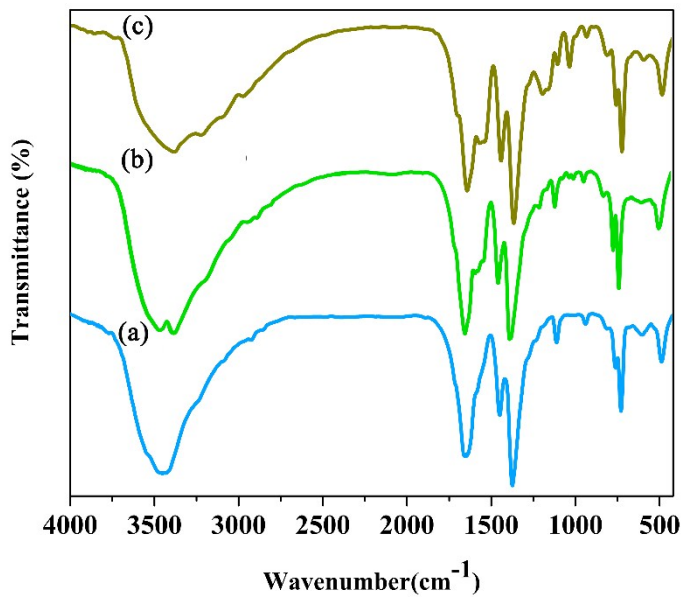


Fig. S1. FT-IR spectra of (a) HKUST (b) HKUST-AMP (c) HKUST-AMP- SO_3H .

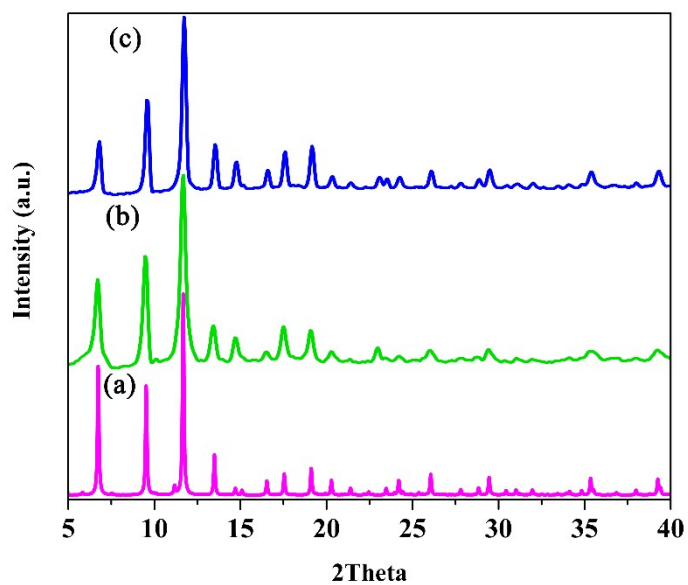


Fig. S2. XRD patterns of HKUST (a) simulated (b) as-synthesized, and (c) HKUST-AMP-SO₃H.

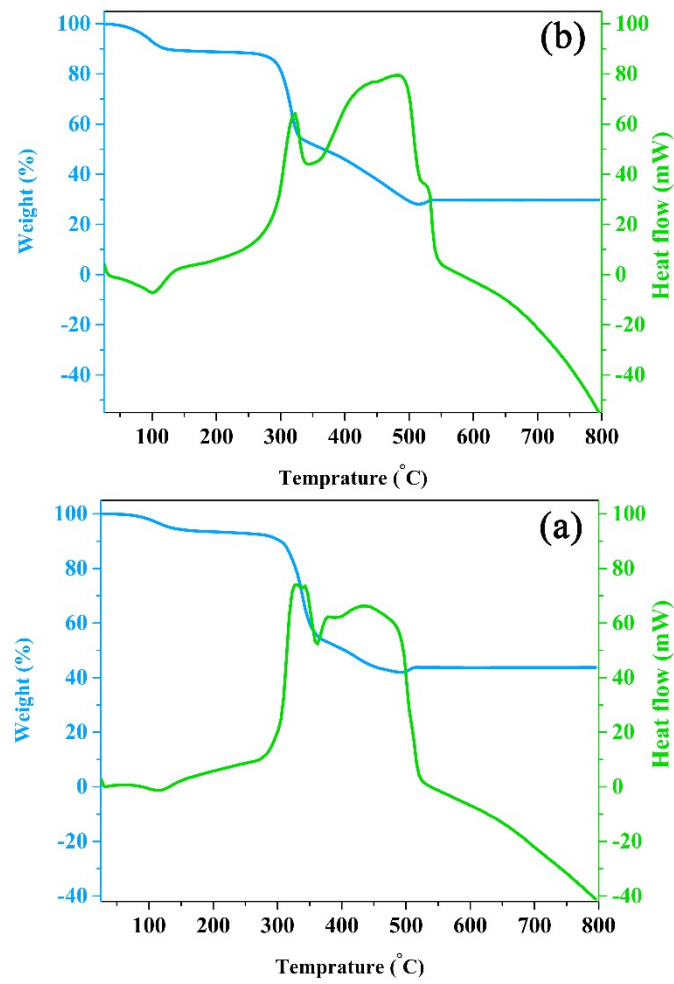


Fig. S3. TGA-DSC curves of (a) HKUST (b) HKUST-AMP-SO₃H.

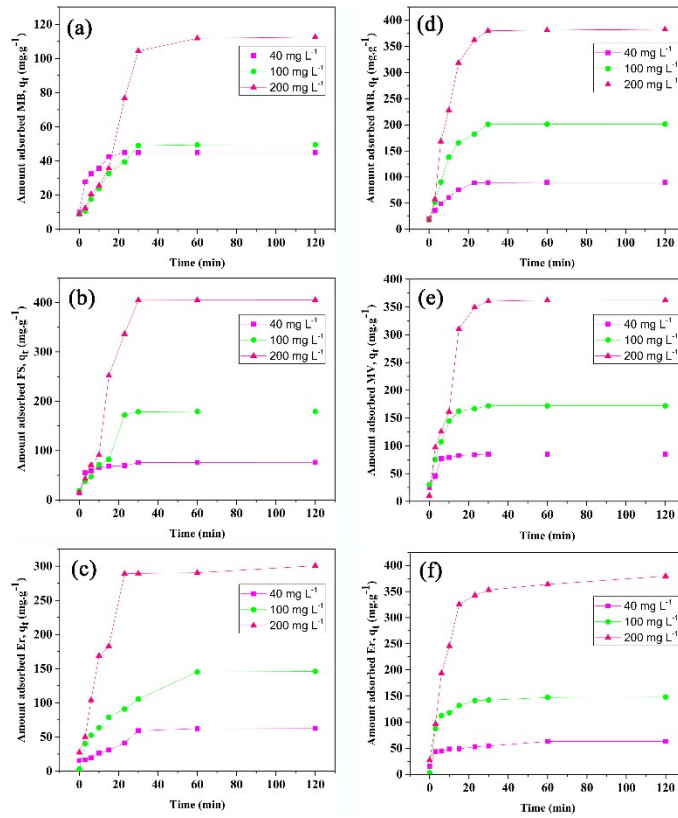


Fig. S4. Adsorption Capacity over HKUST for a) MB, b) FS, and c) Er. Adsorption capacity over HKUST-AMP-SO₃H for d) MB, e) MV, and f) Er.

Table S1. The dye removal percentage of dyes using HKUST and HKUST-AMP-SO₃H in different concentration of dye molecules.

C_0 (mg L ⁻¹)	Dye removal (%)					
	HKUST			HKUST-AMP-SO ₃ H		
	MB	FS	Er	MB	MV	Er
20	64	81	46	97	85	72
40	60	80	42	95	84	71
60	55	79	39	90	83	70
80	51	76	36	87	82	68
100	49	75	31	86	80	65
200	45	73	20	86	78	60

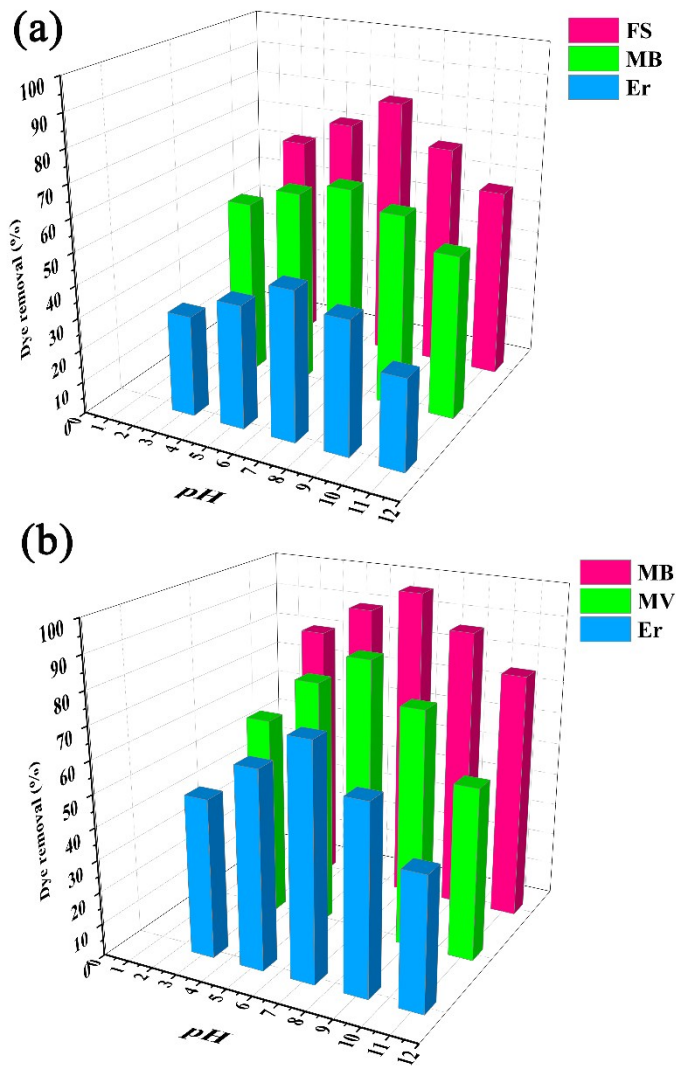


Fig. S5. Effect of pH on dye removal using (a) HKUST (b) HKUST-AMP-SO₃H.

Table S2. The effect of temperature on dye adsorption of MB, FS, Er, and MV over HKUST and HKUST-AMP-SO₃H.

Temperature (K)	Dye removal (%)						
	HKUST			HKUST-AMP-SO ₃ H			
	MB	FS	Er		MB	MV	Er
298	64	81	46		97	85	72
308	50	61	32		72	69	61
323	23	45	17		54	48	43

Table S3. The effect of adsorbent dosage on dye adsorption of MB, FS, Er, and MV.

Dose (mg)	Dye removal (%)					
	HKUST			HKUST-AMP-SO ₃ H		
	MB	FS	Er	MB	MV	Er
3	19	43	20	41	61	39
5	39	66	32	68	76	45
10	64	81	46	97	85	72
15	64	82	48	97	88	74
20	65	84	49	99	89	77

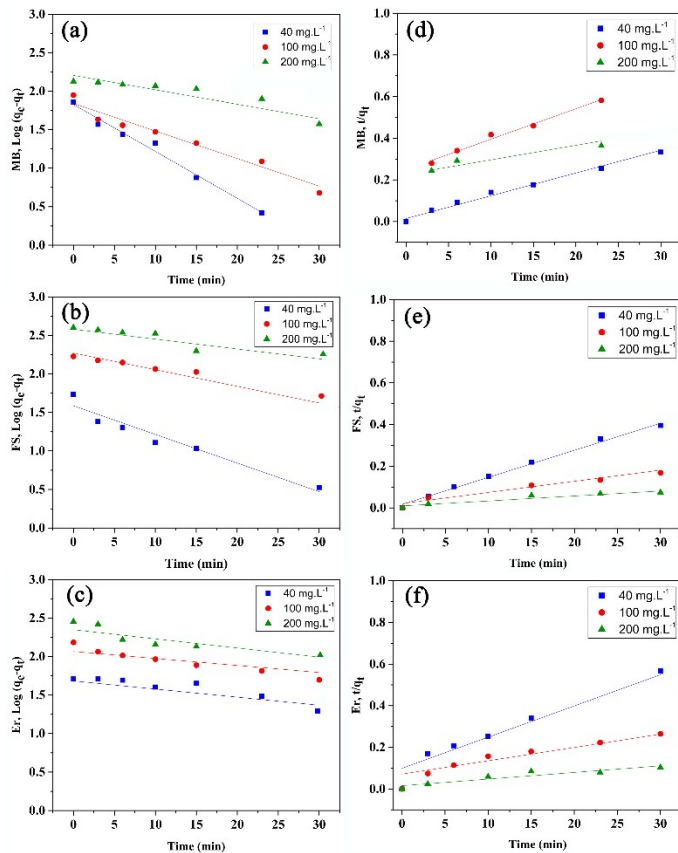


Fig. S6. Plots of pseudo-first-order kinetics over HKUST for a) MB, b) FS, and c) Er. Plots of pseudo-second-order kinetics over HKUST-AMP-SO₃H for d) MB, e) FS, and f) Er.

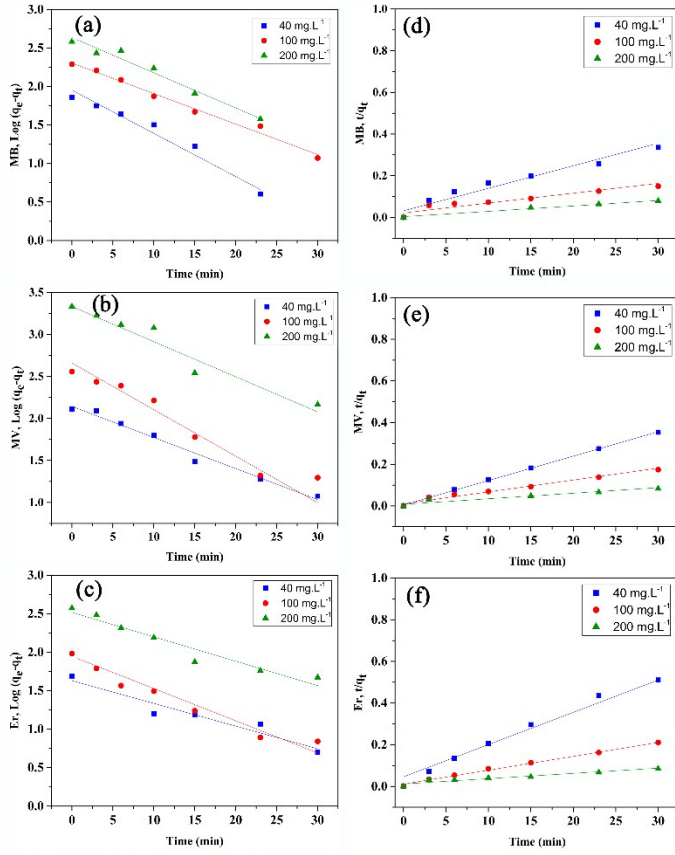


Fig. S7. Plots of pseudo-first-order kinetics over HKUST-AMP-SO₃H for a) MB, b) MV, and c) Er. Plots of pseudo-second-order kinetics over HKUST-AMP-SO₃H for d) MB, e) MV, and f) Er.

Table S4. Adsorption kinetics parameters of MB, FS, and Er using HKUST as adsorbent.

Dye	$C_0(\text{mg L}^{-1})$	pseudo-first-order			pseudo-second-order			
		$K_1(\text{min}^{-1})$	$q_e(\text{mg g}^{-1})$	R_2	$K_2(\text{g mg}^{-1} \text{min}^{-1})$	$q_e(\text{mg g}^{-1})$	R_2	
MB	40	0.140	67.28	0.9849		0.021	91.74	0.9994
	100	0.070	54.18	0.9357		0.011	53.76	0.9893
	200	0.012	128.20	0.973		0.001	142.85	0.9975
FS	40	0.085	38.69	0.9219		2.1×10^{-3}	59.17	0.9996
	100	0.027	125.89	0.849		1×10^{-3}	188.67	0.9911
	200	0.029	380.18	0.9791		0.6×10^{-3}	416.66	0.9930
Er	40	0.024	47.86	0.8626		0.002	66.66	0.9885
	100	0.020	114.81	0.9704		0.5×10^{-3}	156.25	0.9816
	200	0.027	218.77	0.9233		0.6×10^{-3}	312.5	0.990

Table S5. Adsorption kinetics parameters of MB, MV, and Er using HKUST-AMP-SO₃H as adsorbent.

Dye	$C_0(\text{mg L}^{-1})$	pseudo-first-order			pseudo-second-order		
		$K_1(\text{min}^{-1})$	$q_e(\text{mg g}^{-1})$	R_2	$K_2(\text{g mg}^{-1} \text{min}^{-1})$	$q_e(\text{mg g}^{-1})$	R_2
MB	40	0.129	89.61	0.9566	3×10^{-3}	92.59	0.9973
	100	0.091	201.37	0.9874	1×10^{-3}	212.76	0.9942
	200	0.105	425.99	0.988	0.1×10^{-3}	400	0.9993
MV	40	0.002	129.12	0.9434	2×10^{-3}	204.08	0.9999
	100	0.003	153.12	0.9451	3×10^{-3}	175.43	0.9987
	200	0.1275	398.10	0.969	0.3×10^{-3}	370.37	0.9956
Er	40	0.025	24.54	0.9261	0.005	64.51	0.9976
	100	0.096	25.02	0.9235	0.006	149.25	0.9996
	200	0.073	323.59	0.938	0.5×10^{-3}	400	0.9956

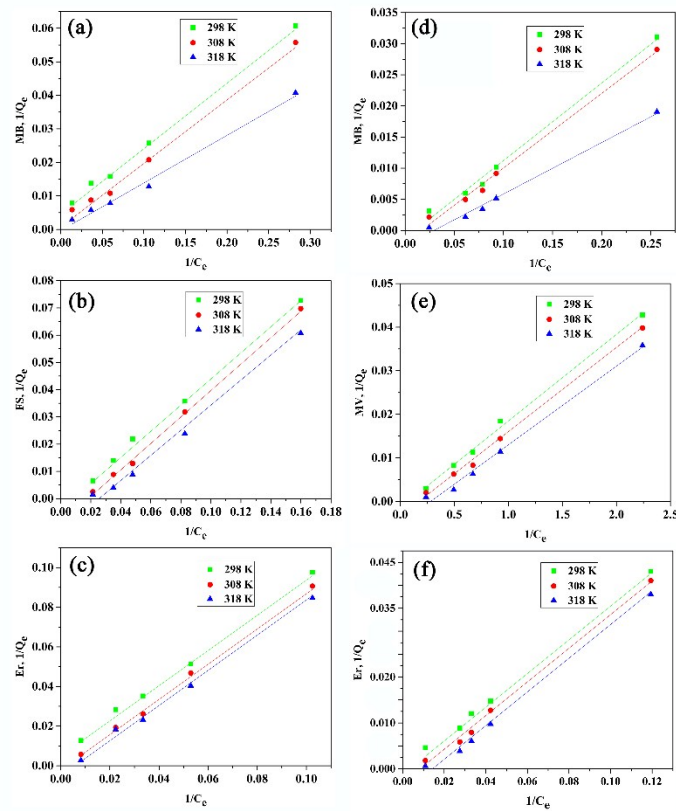


Fig. S8. Langmuir isotherm of adsorption over HKUST for a) MB, b) FS, and c) Er. Langmuir isotherm of adsorption over HKUST-AMP-SO₃H for d) MB, e) MV, and f) Er at 298, 308, 318 °K.

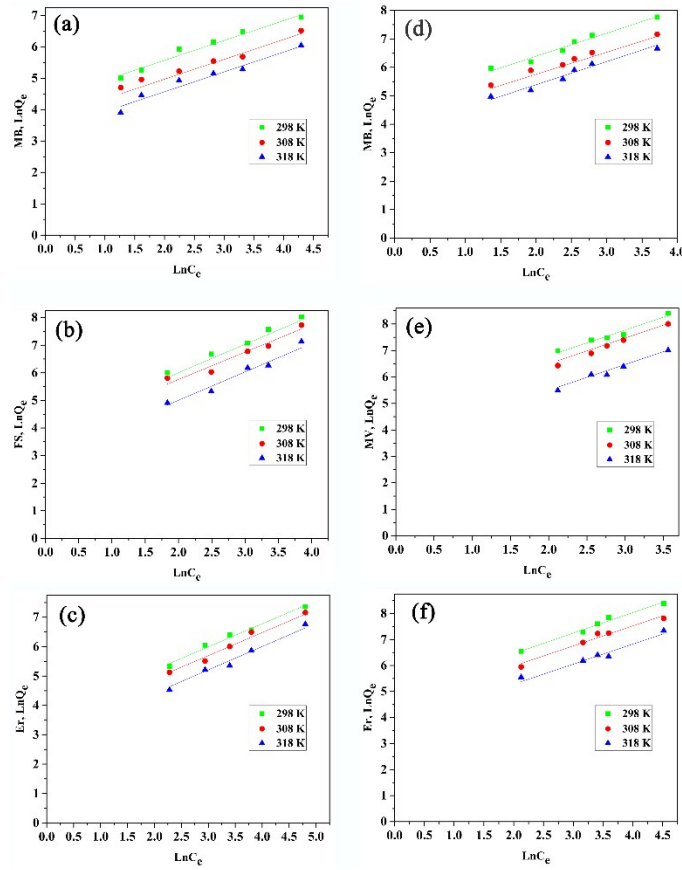


Fig. S9. Freundlich isotherm of adsorption over HKUST for a) MB, b) FS, and c) Er. Freundlich isotherm of adsorption over HKUST-AMP-SO₃H for d) MB, e) MV, and f) Fr at 298, 308, 318 °K.

Table S6. Isotherm parameters of MB, FS, and Er over HKUST.

Dye	T(K)	Langmuir			Freundlich		
		Q(mg/g)	K _L (L mg ⁻¹)	R _L	R ₂	n _F	K _F
MB	298	238.09	0.0214	0.423	0.980	1.620	81.10
	308	224.65	0.0192	0.389	0.991	1.425	80.34
	318	204.21	0.0142	0.354	0.987	1.372	78.12
FS	298	243.90	0.0082	0.627	0.998	0.991	54.99
	308	234.02	0.0072	0.605	0.994	0.990	52.76
	318	210.54	0.0055	0.586	0.991	0.859	50.12
Er	298	200	0.0056	0.709	0.991	1.282	57.64
	308	183.21	0.0045	0.692	0.984	1.204	54.98
	318	176.09	0.0023	0.675	0.995	1.145	52.56

Table S7. Isotherm parameters of MB, MV, and Er over HKUST-AMP-SO₃H.

Dye	T(K)	Langmuir			Freundlich		
		Q(mg/g)	K _L (L mg ⁻¹)	R _L	R ₂	n _F	K _F
MB	298	833.33	0.0096	0.598	0.993	1.240	119.02
	308	810.98	0.0084	0.431	0.986	1.178	110.56
	318	797.45	0.0071	0.367	0.991	1.023	105.98
MV	298	714.28	0.0706	0.201	0.997	1.049	135.74
	308	706.23	0.0695	0.187	0.988	1.023	123.68
	318	695.87	0.0618	0.145	0.992	1.001	109.06
Er	298	833.33	0.0033	0.801	0.994	1.275	133.79
	308	813.98	0.0029	0.765	0.991	1.165	126.25
	318	798.23	0.0021	0.632	0.989	1.078	117.04

Table S8. Thermodynamic parameters of MB, FS, and Er adsorption over HKUST.

Dye	T(K)	$\ln K_0$	ΔG° (kJ mol $^{-1}$)	ΔH° (kJ mol $^{-1}$)	ΔS° (J mol $^{-1}$ K $^{-1}$)
MB	298	1.43	-3.30		
	308	1.40	-2.91	-5.08	-5.09
	318	1.30	-2.73		
FS	298	1.04	-2.52		
	308	0.91	-2.14	-13.35	-36.04
	318	0.70	-1.74		
Er	298	0.65	-1.45		
	308	0.5	-1.19	-12.98	-38.10
	318	0.32	-0.81		

Table S9. Thermodynamic parameters of MB, MV, and Er adsorption over HKUST-AMP-SO₃H.

Dye	T(K)	$\ln K_0$	ΔG° (kJ mol $^{-1}$)	ΔH° (kJ mol $^{-1}$)	ΔS° (J mol $^{-1}$ K $^{-1}$)
MB	298	2.22	-5.40		
	308	1.87	-4.73	-22.56	-57.58
	318	1.80	-4.14		
MV	298	6.12	-4.29		
	308	6.01	-4.13	-10.61	-15.35
	318	5.85	-3.96		
Er	298	1.01	-2.42		
	308	0.89	-2.21	-10.23	-25.89
	318	0.75	-1.89		

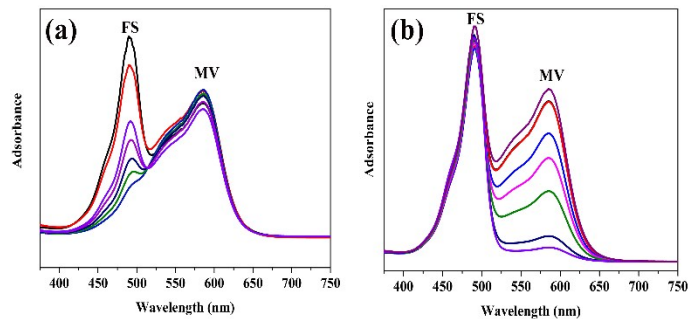


Fig. S10. The reverse performance of (a) HKUST and (b) HKUST-AMP-SO₃H for FS-MV mixture.

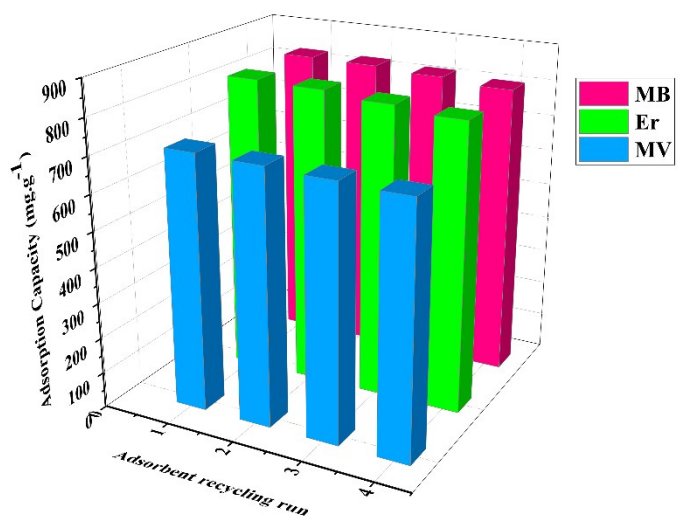


Fig. S11. The effect of recycling run on adsorption of MB, Er, and MV over HKUST-AMP-SO₃H.

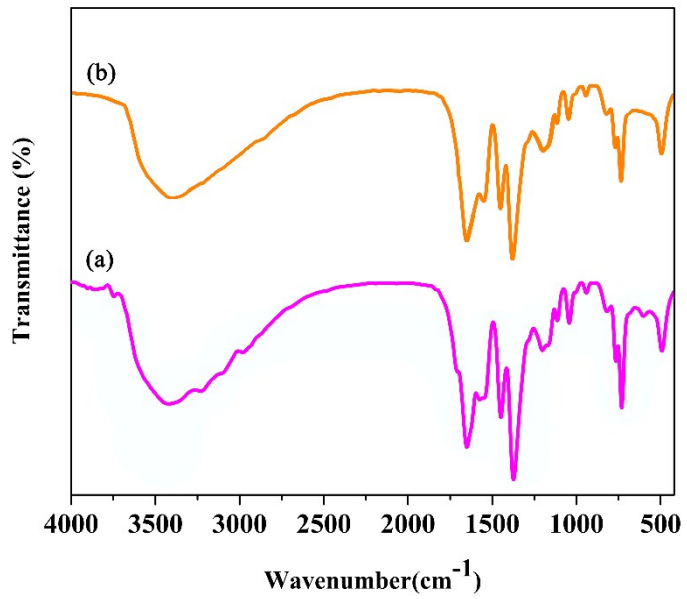


Fig. S12. FT-IR spectra of HKUST-AMP-SO₃H (a) before and (b) after using as an adsorbent.

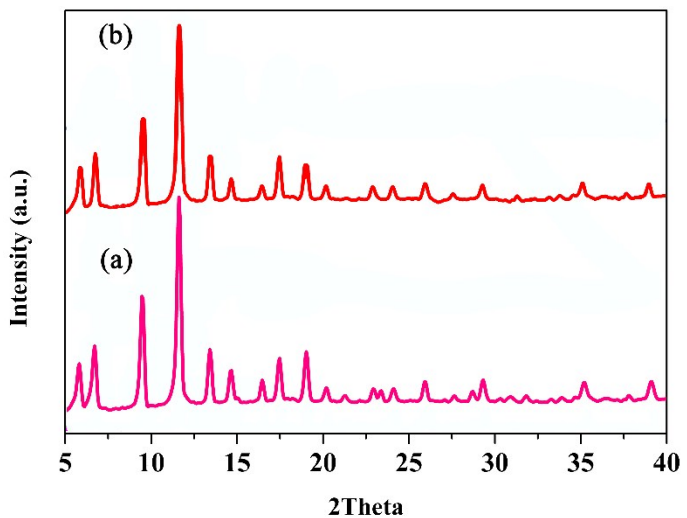


Fig. S13. XRD patterns of HKUST-AMP-SO₃H (a) before and (b) after using as an adsorbent.

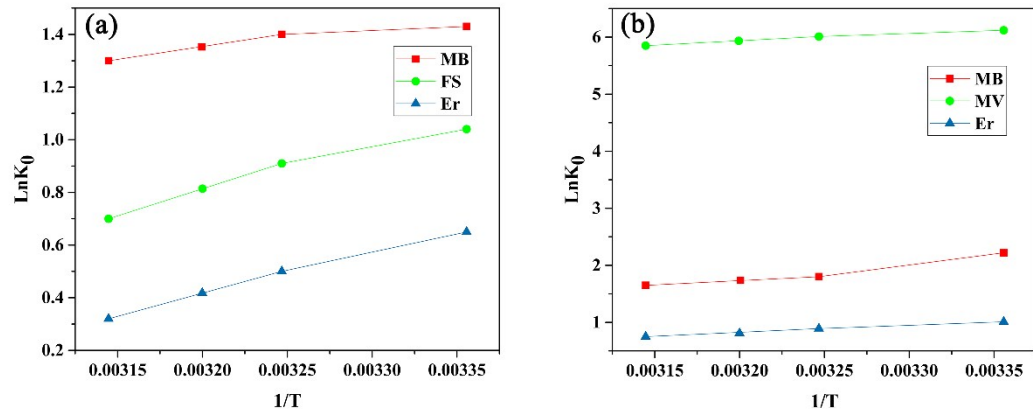


Fig. S14. Van't Hoff plots of used dye molecule over a) HKUST b) HKUST-AMP-SO₃H.